Diagnosis and Classification of Stator Winding Insulation Faults on a Three-phase Induction Motor using Wavelet and MNN

N. Rama Devi
Bapatla Engineering College
Department of Electrical and Electronics Engineering
Bapatla, AP 522102, India

D. V. S. S. Siva Sarma
National Institute of Technology
Department of Electrical Engineering
Warangal, TEL 506004, India

and **P. V. Ramana Rao**
ANU College of Engineering and Technology
Department of Electrical and Electronics Engineering
Nagarjuna Nagar, Guntur, AP 522510, India

ABSTRACT

The growing industrialization needs techniques to diagnose the incipient faults in induction motor at inception stage itself for avoiding the downtime of the production. In this regard detecting the faults in a 3-phase induction motor at an early stage is a vital component in process industries. The condition of the supply unbalance, under voltage and sudden load changes are other involuntary issues which may tend to exhibit current signature similar to the stator winding insulation faults. This paper proposes a robust technique to detect, classify various stator winding insulation faults and severity of stator inter-turn faults when an induction motor works under various operating conditions. In the present work, disturbance features are extracted from three phase residues which are obtained from wavelet multiresolution analysis. Three modular neural networks are implemented, in which one is used to classify various disturbances such as single phasing, supply unbalance, under voltage, stator inter-turn faults, sudden load change and phase faults, second one is used for classifying the stator winding phase faults and third one is used for identifying the faulty phase and severity level of stator inter-turn faults. Simulation and Experimental data demonstrate the validity of the proposed method and improvement in classification accuracy as compared to traditional method.

Index Terms - **Discrete wavelet transform, stationary wavelet transform, stator winding insulation faults, modular neural network, multilayer neural network, sensitivity, specificity.**

1 INTRODUCTION

DEPLOYMENT of an induction motor in process industry is growing day by day due to their low cost, ruggedness, reasonably small size, low maintenance, and operation of an easily available power supply. Even though induction machines are reliable, they are subjected to some undesirable stresses, resulting in faults eventually leading to failures [1]. Several studies have shown that 30%–40% of induction motor failures are due to the stator winding breakdown [2-3]. The requirement for condition monitoring has increased recently because of the widespread use of automation and consequent reduction in direct man-machine interface to supervise the system operation. Condition monitoring is a good graphical trend of the machine parameters for the purpose of detection, analysis, and correction of the machine problems before the failure takes place. This may help to increase the machine availability and performance, reducing consequential damage, increasing machine life, reducing spare

Manuscript received on 1 August 2015, in final form 20 June 2016, accepted 30 June 2016.

DOI: 10.1109/TDEI.2016.005576

parts inventories, and reducing breakdown time [4]. Normally, the deterioration of stator winding insulation usually begins with an inter-turn fault which produces a high circulating current between adjacent coils and hence burns the insulation in adjacent windings. This insulation failure expands to the core very fast leading to stator to core insulation failure. Hence, reliable detection techniques are essential for detecting the stator insulation failure at the earliest to avoid catastrophic motor failures [5]. A well-known technique to detect inter-turn short circuits in time domain analysis is based on the presence of negative sequence components of stator currents [6], which is the first developed technique for detecting the stator winding failure. Detection of stator faults using dq0 components [7], the envelope of the stator currents [8], the stator currents in multiple reference frames [9] and wavelet transform of the stator currents [10] are just alternative representations of the same current components. Fault detection using induced voltage at motor terminals when the power supply is turned off is proposed in [11], but this method cannot provide continuous monitoring and protection. In [12] a review and summary of various online inter-turn fault diagnosis strategies for electrical machines with a focus on PM machines is presented. The stator winding faults create unbalancing in the line currents, and similar unbalancing is also created due to asymmetrical winding resistances and supply unbalances [2, 3, 5, 13, 14]. Some work has been done to distinguish the unbalancing due to faults and the unbalancing due to the inherent asymmetry in the winding and supply [15, 16]. However, the distinction between these two phenomena is highly challenging under no-load conditions. This is one of the major issues in recent times and another is the identification of low-level severity of stator inter-turn faults (1 or 2 turn failures) under various operating conditions. Recently, significant efforts have been made to the use of artificial intelligence tools to develop condition monitoring and fault diagnostic techniques for electric machines to segregate the faults. Artificial intelligence techniques are considered significant in condition monitoring and fault diagnosis of electrical machines as reviewed in [17]. Neural network and fuzzy logic techniques have their own shortcomings as discussed in [18] and thus a specific combination of these two techniques, known as Adaptive Neuro-Fuzzy Inference System (ANFIS), have been developed as a better alternative solution [19]. The ANFIS technique offers the best training feature of the neural network and heuristic interpretation of the process results similar to fuzzy logic theory, thus providing a powerful tool that can be employed in conjunction with the condition monitoring and fault diagnostic applications. The use of ANFIS is growing in popularity in this niche application area and a significant amount of literature is available [20-22]. Bearing fault and inter-turn insulation failure of main winding of a single-phase induction motor is considered in [23]. Stator current, rotor speed, temperature of the winding, bearing temperature and motor noise are considered as inputs to the ANFIS. However, additional noise sensors are not very reliable and the data collected from such sensors is not very accurate. Classification of more faults with a single parameter is more complicated than multiple parameters. Modular Neural networks (MNN) have remarkable ability to derive meaning from complicated or imprecise data and can be used to extract patterns and detect trends that are too complex. Such an approach has noticeable advantages of simple and reduced architecture and better learning capability [24-25]. The work reported so far in the literature has confined to detection and classification of only two or three types of faults. However, a single reliable procedure for any type of stator winding faults and supply side faults based on non-invasive signals is not in the literature.

This paper proposes the application of Wavelet and MNN based fault detection and classification scheme for stator winding insulation faults. Unbalancing condition at the motor could be due to stator winding insulation faults or due to other conditions. In this paper, a robust diagnosis procedure is proposed to classify the stator winding insulation faults from other disturbances such as single phasing, supply unbalance, under voltage and sudden load change. The proposed method requires only three measurements and thirteen features. The three phase stator currents are the three measurements and are sensed for each of the disturbance and normal cases. These three phase currents are analyzed with wavelet transform to detect the disturbance instant. Three statistical features of second level approximate coefficients of three phase values are considered as inputs to the first classifier for classifying the various disturbances on a 3-phase induction motor. To identify the faulty phase and severity level of stator inter-turn faults another modular neural network is considered. To make the identifier insensitive to the operating conditions the network is trained with input features of three-phase detail level coefficients and ratio of the post and pre-fault mean values of 4^{th} level approximate coefficients. To classify the stator phase faults one more modular neural network is considered and trained with inputs of three-phase detail coefficients only for making the proposed scheme more generalized. The proposed detection and classification scheme is effective in classifying and identifying the stator winding insulation faults.

2 MODELLING AND SIMULATION

Conducting numerous experiments on a practical machine to study the behavior of faults is not feasible, as it can lead to the destruction of the machine. To study the behavior of the motor under stator inter-turn fault conditions requires a simple and reliable model. In this paper, a low to high-frequency model is considered, to analyze the stator inter-turn faults. In medium to high-frequency ranges, a distributed parameter model is the best for analyzing the motor behavior. Compared to low-frequency model, the distributed parameter model requires extra elements as shown in Figure 1. The additional parameters of the distributed model are calculated from the differential mode and common mode tests which have been discussed in [26]. In general, distributed parameters are determined by measuring the frequency response from differential mode (DM) test setup and common mode (CM) test setup. A three-phase, 3-hp, 440 V, 4 pole 50 Hz Induction Motor with 36 slots, 6 coils per phase and 72 turns per coil is considered in the present study. The DM test was performed by connecting an LCR meter between phase A and

tied leads of phase B and phase C. This test procedure is recommended for an ungrounded motor frame and LCR meter in Z-θ mode. The CM test was performed with ground frame as one probe and phase A, phase B and phase C motor leads tied together to form the second probe to LCR meter in Z-θ mode. Figure 2 shows the experimental setup of a three-phase 3-hp induction motor. Table 1 presents the low to high-frequency parameters of a 3-hp induction motor. To validate the model, the frequency responses obtained from the experimental setup are compared with those from simulation. Figures 3a and 3b show the comparison between measured and simulated frequency responses in both DM and CM. These figures demonstrate that the frequency response observed in simulation closely matches with response measured on the practical machine. Hence, the model is valid for transient studies.

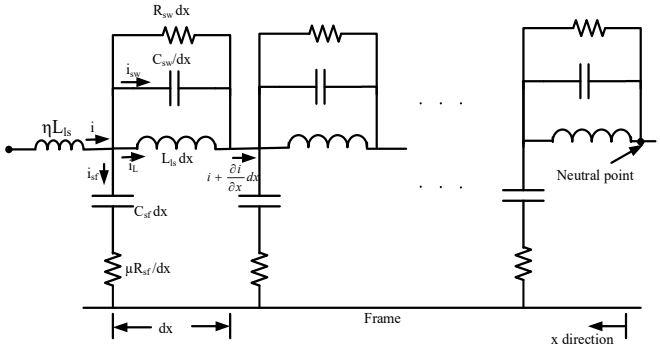

Figure 1. Distributed parameter model of a three-phase induction motor.

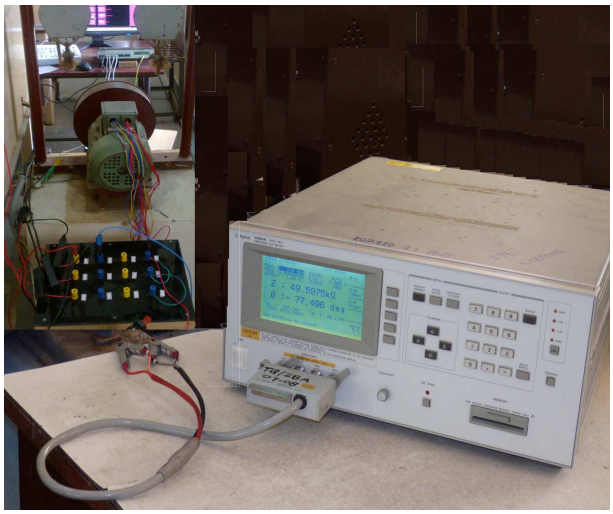

Figure 2. Experimental setup of a 3-hp three-phase induction motor

Table 1. Low and High Frequency Parameters of a three-phase 3-hp Induction Motor.

Parameters	Values	Obtained from
Stator Resistance (R_s)	9.1 Ω	No load and Blocked rotor Test
Stator Leakage Inductance (L_{ls})	41.38 mH	
Rotor Resistance (R_r)	8.08 Ω	
Rotor leakage inductance (L_{lr})	31.83 mH	
Magnetizing Inductance (L_m)	904.44 mH	
Core Resistance (R_{core})	2842.8 Ω	
Stator to frame capacitance (C_{sf})	0.253 nF	Differential Mode and Common mode test
Anti-resonance resistance (μR_s)	2.667 Ω	
Anti-resonance leakage inductance (ηL_{ls})	3.547 μH	
Stator turn to turn capacitance (C_{sw})	0.853 nF	
Stator turn to turn damping resistance (R_{sw})	17356 Ω	

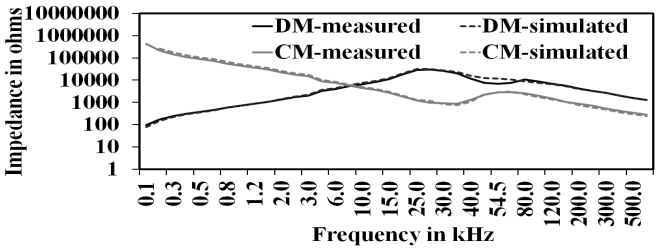

(a)

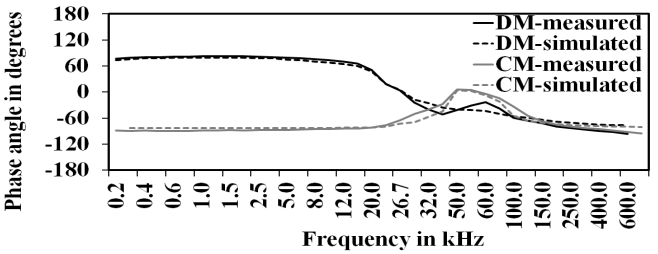

(b)

Figure 3. Frequency responses in DM and CM (a) measured and simulated magnitude responses in DM and CM (b) measured and simulated phase responses in DM and CM.

3 SIMULATION MODEL FOR STATOR FAULTS

To simulate the stator inter-turn faults a 3-phase, 3-hp, 415V, 50 Hz induction motor with a star connected stator winding is considered. The stator winding corresponding to the phase in which the fault is created is divided into two parts. An additional branch is connected in parallel to the rotor resistance to simulate the disturbance component due to stator inter-turn fault. The fault is created by closing three switches as shown in Figure 4 and it illustrates the stator inter-turn fault in R-phase of a 3-phase induction motor. In this figure Part 1 refers to a healthy portion of the winding and Part 2 refers to the shortened turns of the winding. The resistance, inductance, and insulation capacitance are divided in proportion to the number of short-circuited turns. The various percentages of turn level short circuits in different phases have been simulated in the MATLAB/Simulink environment. In the case of stator turn-turn faults, the switches S1 and S2 are connected between phases and if it is a stator turn to ground fault the switches S1 and S2 are connected between phase and ground. To bring the simulation model more close to practical scenarios, Gaussian noise is injected in each phase. The noise level to be injected is calculated from the captured three-phase stator currents in the experimental setup. Totally 9 types of stator faults are considered for simulation such as stator inter-turn fault in R phase, Y phase, B phase, stator turn-turn fault between RY phases, YB phases, BR phases and stator turn-ground fault in R phase, Y phase, B phase.

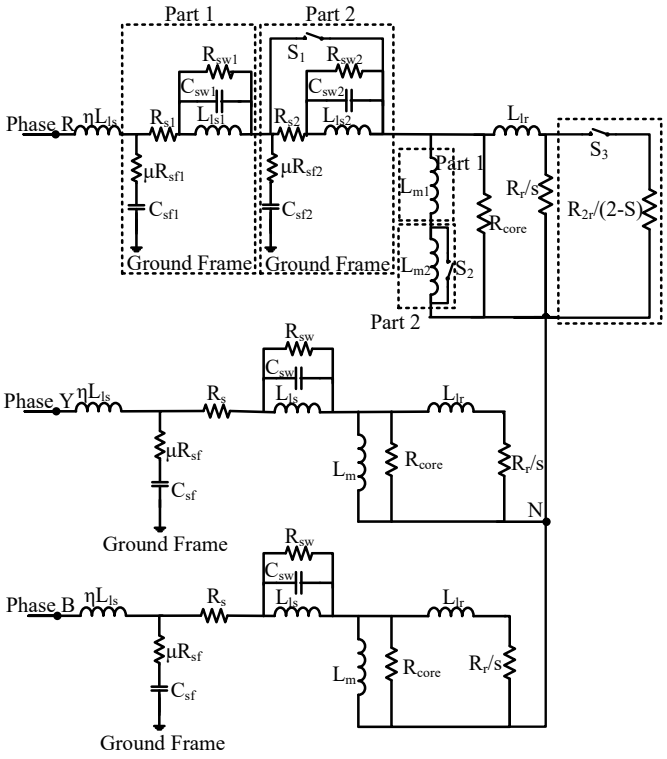

Figure 4. Stator inter-turn fault simulation model for a 3-phase induction motor.

4 EXPERIMENTAL SETUP

An experimental setup was prepared with a 3-phase, 3-hp, 4 pole, 50 Hz, 415 V induction motor with 36 slots, 6 coils per phase and 72 turns per coil. In order to create the inter-turn short circuit, two tapping points are taken out per phase from the neutral of the stator winding. Each tapping is having a resistance of 0.8 ohms. The stator inter-turn faults are created experimentally by connecting a suitable resistance between tapping point and ungrounded neutral [6-7]. If the fault is a turn-turn or turn to ground then suitable resistance is connected between tapping point of one phase to another or phase to ground. Another rating of 10-hp induction motor is also considered for creating various stator faults for a level of 2 turns to 8 turns in steps of 2 turns without connecting any resistance between tapping point and neutral of the stator winding as in this case tapping points are directly taken to the level of 2 turns. Totally 6 types of disturbances are created make use these machines. Figures 5a and 5b show the experimental setup for creating various disturbances on a 3-hp and 10-hp induction motors respectively. In the proposed method, three-phase stator currents are captured in 1 Sec with a sampling frequency of 6.6 kHz by using UNIPOWER DIP 8000 network analyzer. To acquire the signals the network analyzer is connected to a personal computer.

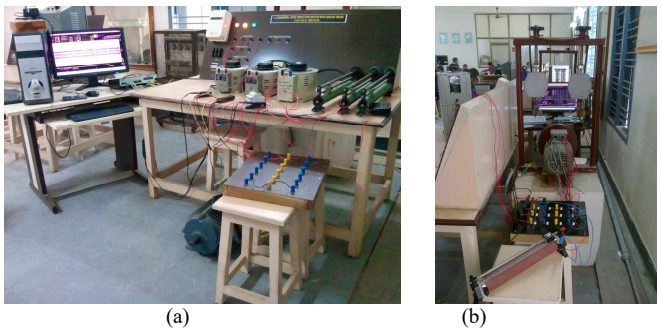

(a) (b)

Figure 5. Experimental setup for creating the faults on (a) 10-hp induction motor (b) 3-hp induction motor.

5 NOISE ELIMINATION USING SWT

Wavelet Transform (WT) is an efficient means of analyzing transient currents and voltages. Discrete Wavelet Transform (DWT) is the most popular wavelet transform. It is widely used in power engineering applications, especially in protection systems for detection, identification, classification and localization of the power system disturbances both in time and frequency domains [27]. A threshold is used in wavelet domain to smooth out or to eliminate some coefficients of WT of the measured signal. The noise content of the signal is reduced effectively under the non-stationary environment, but the results obtained from it are not the optimal mainly due to the loss of the invariant translation property [28]. To overcome this deficiency of DWT, Stationary wavelet transform (SWT) can be used. The SWT is also similar to the DWT in that the low-pass and high-pass filters are applied to the input signal at each level, in which the downsampling stage at each scale is replaced by an upsampling of the filter before the convolution.

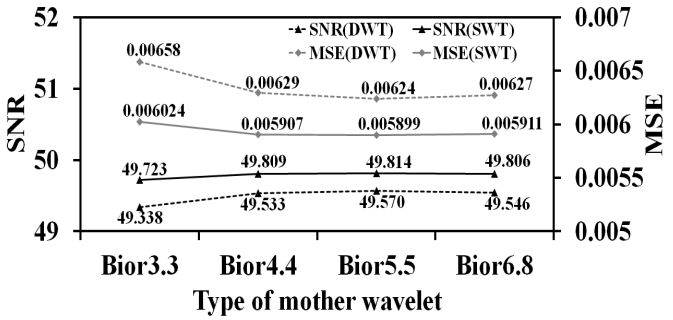

Figure 6. Variation in SNR and MSE values for different mother wavelets of biorthogonal family.

In the proposed technique, Bior5.5 wavelet has been used as the wavelet basis function for fault detection and identification. Initially DWT with different mother wavelets is applied for signal reconstruction and the best performance is observed by using biorthogonal family of mother wavelet. Hence, the advantage of SWT over the DWT in signal reconstruction is explained by applying different wavelets of biorthogonal family and calculating mean square error (MSE) and signal to noise ratio (SNR) between the reference signal and reconstructed signal of stator current in phase R. Figure 6 show the MSE and SNR for different wavelets of bi-orthogonal family. Results clearly demonstrate that SWT is far better than DWT in the application of noise elimination or signal reconstruction and Bior5.5 mother wavelet has less MSE compared to others.

6 PROPOSED DETECTION AND CLASSIFICATION TECHNIQUE

The proposed fault detection and classification technique starts with data acquisition and then application of wavelet analysis and classification. This is illustrated in Figure 7. The threshold based reconstruction of the three-phase stator currents should compensate the effects due to supply unbalance and machine unbalance. The reconstructed three phase current signals are obtained by using stationary wavelet denoising technique of level based threshold. The three-phase currents of the motor are decomposed with SWT of Bior5.5 to obtain approximate and detail level coefficients up to 6th level. The thresholds of d1 coefficients to d4 coefficients are made maximum while threshold value of d5 coefficients is set to a high value as this band of frequency components is sensitive to the supply unbalances. The threshold value of d6 is calculated based on its peak value in the 1st cycle and multiplied with a distortion factor which is calculated from RMS value of the current signal during start-up (preferably in the 1st cycle). The threshold value of d6 coefficient may enhance the fault signature because the pre-fault value is subtracted from the captured signal. Therefore, the reconstructed signals are called as fault residues. This type of reconstruction is essential especially if fault feature is very close to the noise level.

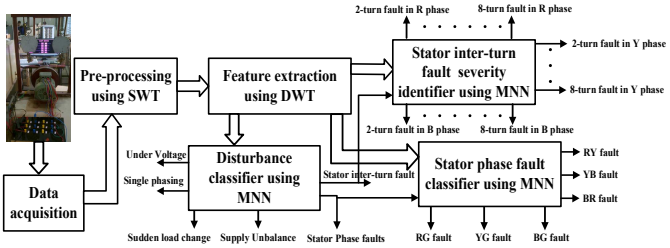

Figure 7. Proposed stator fault detector and classifier

6.1 FEATURE EXTRACTION

A short circuit between the turns in a stator winding causes an unbalance in stator currents. These unbalances cannot be seen directly from the three-phase stator currents if the level of turn short circuit is too small i.e. 1 or 2 turns. Figures 8a and 8b show the three-phase stator currents for 2-turn short circuit in R-phase of a 3-hp induction motor under experimental and simulation cases respectively. From these figures, the unbalance due to stator inter-turn short circuit is not predictable by eye due to the noise and supply or machine unbalances. Hence, an efficient pre-processing method is required for extracting the fault residues and instant of fault even though the motor is operated under noisy environment. In this regard, time-frequency domain analysis of SWT is considered and carried out in MATLAB/Simulink environment for predicting the fault residues. Figures 9a and 9b, show the three-phase residues based on minimax method and proposed threshold based method (mentioned in above section) for 2-turn short circuit in R-phase under experimentation. Similarly, Figures 9c and 9d show the simulation cases of three-phase residues based on minimax method

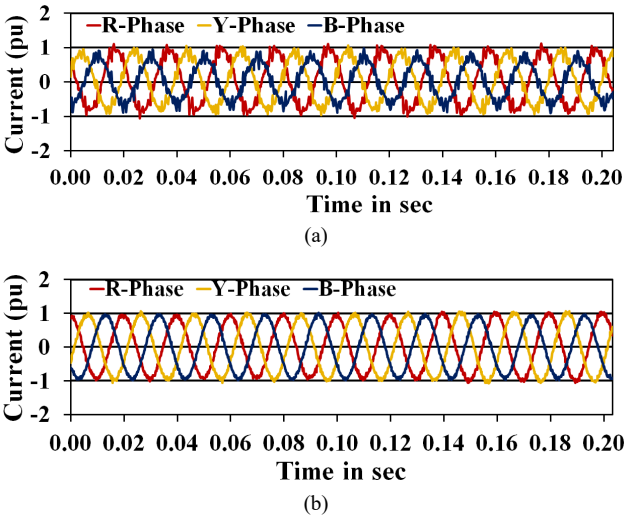

Figure 8. Three-phase stator currents for 2-turn short circuit in R-phase of 3-hp induction motor under (a) experimentation (b) simulation.

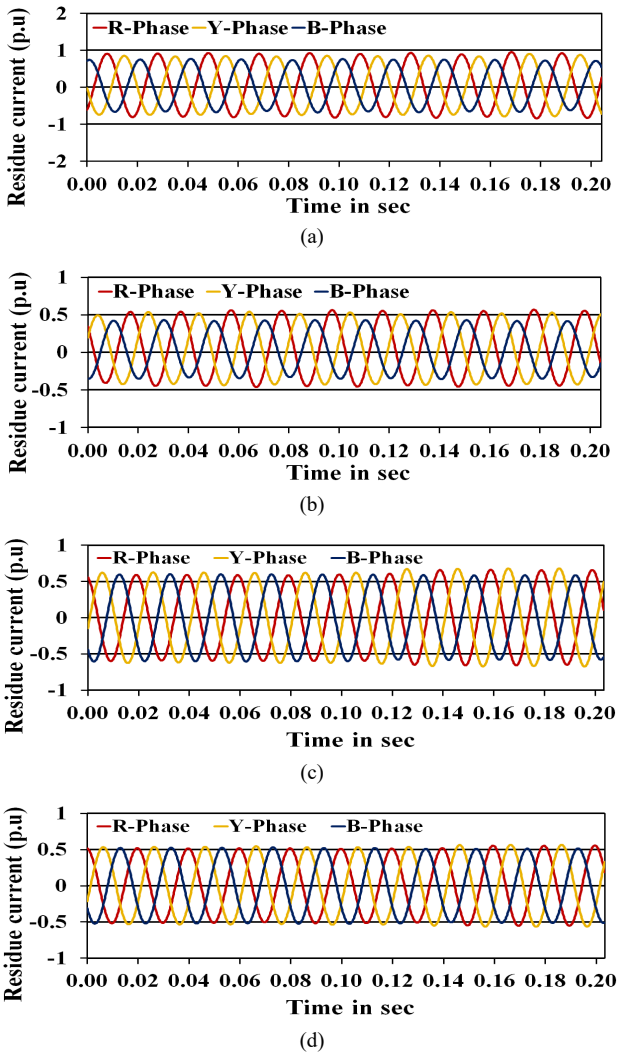

Figure 9. Three-phase residues for 2-turn short circuit in R-phase (a) level based minimax method applied for experimental case (b) proposed threshold method applied for experimental case (c) level based minimax method applied for simulation case (d) proposed threshold method applied for simulation case.

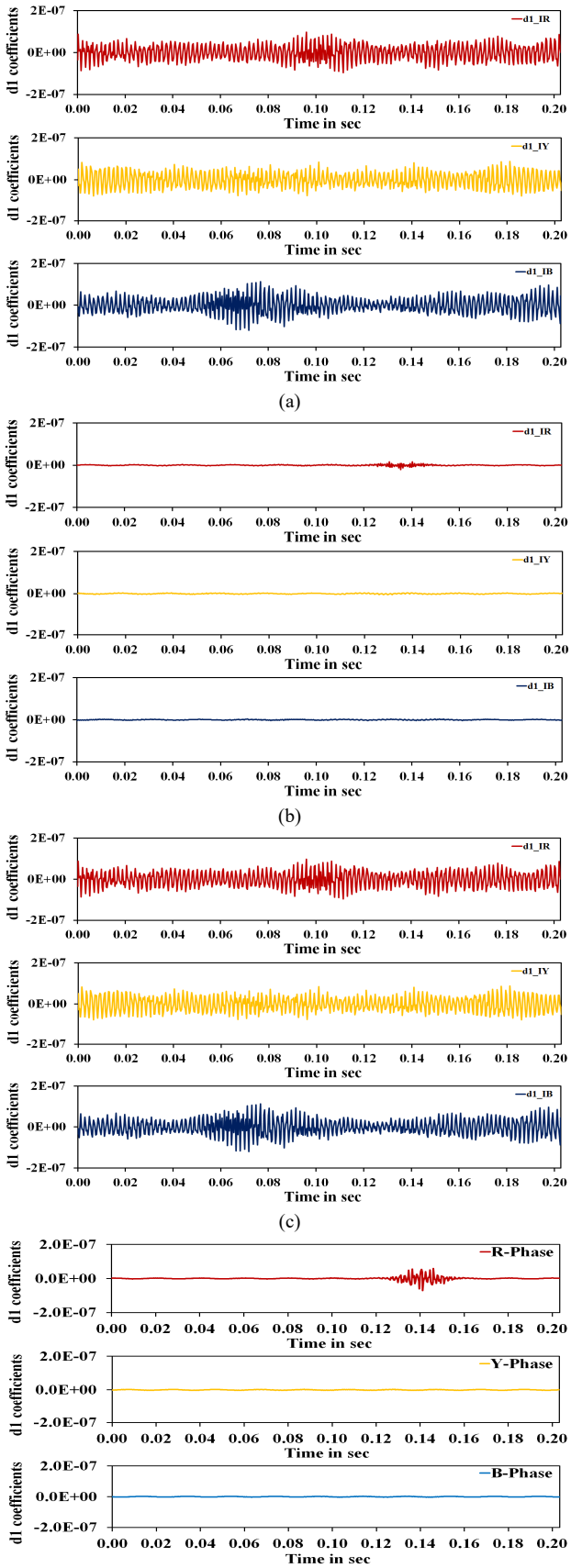

Figure 10. Variation in detail level coefficients for 2-turn short circuit in R-phase (a) level based minimax method applied for experimental case (b) proposed threshold method applied for experimental case (c) level based minimax method applied for simulation case (d) proposed threshold method applied for simulation case.

and proposed method respectively. From the waveforms, the identification of the fault instant is not possible. Hence, once again the reconstructed signals are decomposed by using DWT of Bior5.5 mother wavelet. To extract the fault features the three-phase residues are decomposed up to 4^{th} level. Figures 10a and 10b demonstrate the experimental cases of detail coefficients of residues based on minimax method and proposed method respectively. Similarly, Figures 10c and 10d show the simulation cases of detail coefficients of residues based on minimax method and proposed method. The variation in detail level coefficients in Figures 10b and 10d have clearly demonstrated that the proposed wave reconstruction and decomposition is superior than the existing method to extract the fault features and its instant. The variation in three-phase detail level coefficients exists throughout the interval if decomposed signal is reconstructed with minimax method. Hence, fault feature extraction and instant of fault identification are not possible by using minimax method. In this paper, the abnormal condition of the induction motor can be detected by checking three consecutive fault indices values with an adaptive threshold *Th* and count value of these fault indices over a window of 10 samples should be greater than 6. The fault index (I_f) is described mathematically as follows.

$$I_f(n) = \left|slope\_d1I_R(n)\right| + \left|slope\_d1I_Y(n)\right| + \left|slope\_d1I_B(n)\right| \quad (1)$$

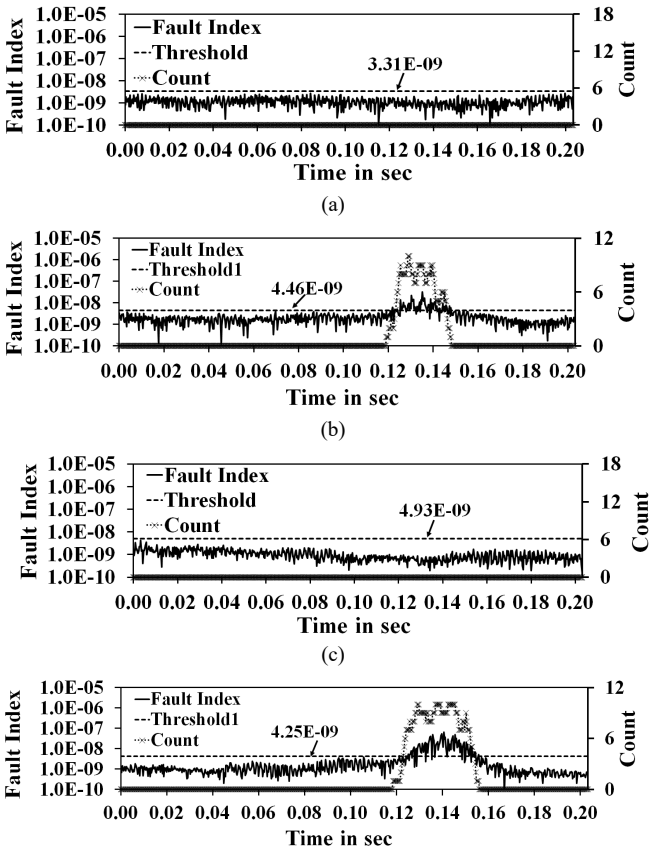

Figure 11. Variations in fault indices and count values of a 3-hp induction motor for (a) experimental case of healthy (b) experimental case of 2-turn short circuit (c) simulation case of healthy (d) simulation case of 2-turn short circuit.

Table 2. Comparison of detection criteria for stator inter-turn faults in R-phase of experimental and simulation cases on a 3-hp induction motor

Type of Disturbance	Experimental		Simulation	
	RMFI	RTH	RMFI	RTH
2-turn fault in R-phase	34.33	1.35	23.20	0.86
4-turn fault in R-phase	76.40	3.33	84.78	1.79
6-turn fault in R-phase	133.81	4.31	124.39	3.27
8-turn fault in R-phase	282.12	3.27	217.55	2.98
2-turn fault in R-phase with 2% SUB	19.59	0.84	10.33	0.72
4-turn fault in R-phase with 2% SUB	69.67	3.18	61.09	3.68
6-turn fault in R-phase with 2% SUB	121.13	7.59	114.86	4.12
8-turn fault in R-phase with 2% SUB	170.34	4.11	127.25	4.11
2-turn fault in R-phase with 50% load	31.09	9.03	34.09	3.96
4-turn fault in R-phase with 50% load	99.45	6.35	81.17	3.57
6-turn fault in R-phase with 50% load	74.25	8.34	75.36	3.29
8-turn fault in R-phase with 50% load	126.07	2.75	189.12	2.69

RMFI: Relative value of maximum fault index (w.r.t. normal)
RTH: Relative value of adaptive threshold (w.r.t. normal)

Table 3. Comparison of detection criteria for various abnormalities of experimental and simulation cases on a 3-hp induction motor

Type of Disturbance	Experimental		Simulation	
	RMFI	RTH	RMFI	RTH
4-turn phase fault between RY phases	206.44	3.01	469.02	2.28
6-turn phase fault between RY phases	379.92	4.69	356.28	0.96
8-turn phase fault between RY phases	269.48	8.20	603.89	5.02
4-turn ground fault in R-phase	74.07	10.8	107.02	4.24
6-turn ground fault in R-phase	143.52	6.83	356.11	5.76
8-turn ground fault in R-phase	169.30	4.68	304.53	4.10
Single phasing in R-phase	812.78	3.66	899.34	3.67
Single phasing in Y-phase	474.06	5.16	624.59	6.48
Single phasing in B-phase	551.00	4.42	573.86	8.67
3% Supply unbalance in R-phase	144.57	5.23	81.74	2.82
3% Supply unbalance in Y-phase	166.19	5.50	84.01	0.35
3% Supply unbalance in B-phase	159.20	4.31	93.30	2.78

RMFI: Relative value of maximum fault index (w.r.t. normal)
RTH: Relative value of adaptive threshold (w.r.t. normal)

To validate the proposed detection criteria, a 3-hp induction motor is considered and various abnormalities are simulated in MATLAB/Simulink environment. The same abnormalities are also created on a 3-hp induction motor using experimental setup. Especially, stator inter-turn faults are created under certain loaded conditions such as 0%, 50% and 100%. Stator inter-turn faults are also created experimentally on no-load condition with minor supply unbalances like 1%, 2%, and 3%. In case of simulation that is extended up to 5% due to numerous data required for classification. Figures 11a, 11b, 11c and 11d represent the variation in fault indices and count values for healthy and 2-turn short circuit in R-phase of experimental and simulation cases respectively. The results illustrate that the fault indices are below the adaptive threshold when the motor is under healthy condition. Apart from healthy condition, the fault indices are above the adaptive threshold and count values are also more than 6. The detection criteria for both experimental and simulation cases of different levels of stator inter-turn short circuits under balanced supply, 3% of supply unbalance and 50% of loaded conditions are illustrated in Table 2. Table 3 shows the detection criteria for remaining abnormal conditions of both experimental and simulation cases. The results of Table 2 and Table 3 depict the correctness of proposed detection criteria for various abnormalities of experimental and simulation cases of a three-phase 3-hp induction motor. To check the reliability of the proposed detection criteria, another rating of 10-hp induction motor is also considered. Figures 12a 12b, 12c and 12d demonstrate fault indices along with adaptive threshold *Th* under various experimental cases on a 10-hp induction motor of healthy, 2-turn fault, under voltage and supply unbalance conditions respectively. From these results it is clear that the proposed algorithm has successfully detected the abnormal conditions of the motor. To classify all these abnormalities certain features are essential for separating them. In this totally 9 features of 2nd level approximate coefficients are taken over a window of 1 cycle from the fault instant to classify the disturbances. Figure 14 illustrates the variation levels of feature 1, feature 2 and feature 3 for various disturbances. For further classification, four more features of detail level coefficients are required for classifying the stator winding insulation faults along with faulty phase and severity level of stator inter-turn faults. The following section explains the various classifications.

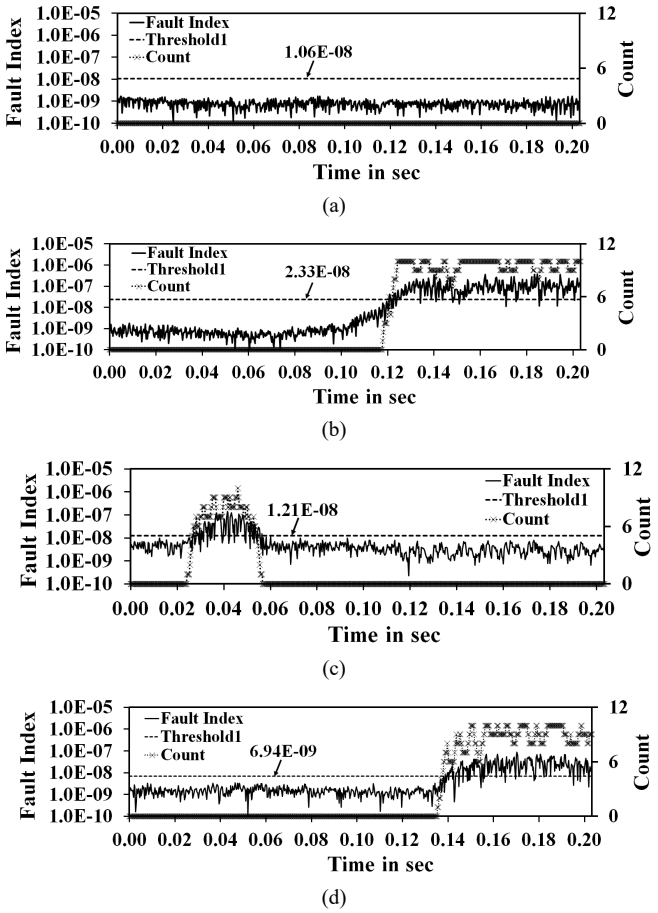

Figure 12. Variations in fault indices and count values of a 10-hp induction motor for various experimental cases: (a) healthy (b) 2-turn short circuit (c) under voltage (d) supply unbalance

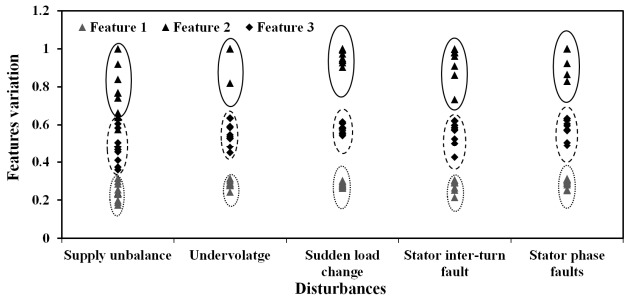

Figure 13. Variation in features for various disturbances.

6.2 ANN STRUCTURES FOR STATOR FAULTS CLASSIFICATION

Artificial neural networks are divided into two main categories viz monolithic networks and modular ones. In canonical implementations, most systems employ a monolithic network in order to solve the given task. However, when a system needs to process large amounts of data or when the problem is highly complex, then it is not trivial, and sometimes unfeasible, to establish a good architecture and topology for a single network that can solve the problem. In order to overcome some of the aforementioned shortcomings of monolithic ANNs, many researchers have proposed modular approaches [29-30]. One of the major benefits of a modular neural network is the ability to reduce a large, unwieldy neural network to smaller, more manageable components. Other benefits of these networks are their efficiency, lower required training time and robustness. In this paper, three modular multilayer neural networks are implemented to classify various faults on a three-phase induction motor, identify various stator winding insulation faults and severity level of stator inter-turn faults. The performance is compared with artificial neural network (ANN) of a single multilayer neural network and double multilayer neural network through the simulation and experimentation. Figure 14 shows the schematic diagram for classification of stator faults using ANN. In this paper three ANNs are constructed for classifying the stator winding insulation faults and severity of the fault in case of stator inter-turn faults. In this the first one is for classification of type of disturbance (ANN-1), the second one is for identification of faulty phase and severity level of stator inter-turn faults (ANN-2) and the third one is for classification of stator winding phase faults (ANN-3). Figure 15 shows the schematic representation of classifiers using ANN. This approach decreases the training time as ANN-2 and ANN-3 train only when the disturbance classifier recognizes the disturbance as related to the stator winding insulation faults which means that the faults are related to stator inter-turn and stator phase faults only. In this paper, each ANN is modeled as a feed forward multilayer back propagation network. The inputs to the ANN-1 are the statistical features of second level approximate coefficients of three-phase residue currents, which are standard deviation, maximum value and mean value obtained over a window of one cycle from the fault instant. The output of ANN-1 gives 6 classes (C_1–C_6) of different types of induction motor disturbances and these are as follows:

C_1→Single phasing C_2→Supply unbalance

C_3→Under voltage C_4→Sudden load change

C_5→Stator inter-turn fault C_6→Stator phase fault

The slope of detail level coefficients of absolute peak values of three phase residue currents are fed as inputs to the ANN-2 and ANN-3 when it is activated. One more additional input is required for ANN-2 for identifying the severity of the stator inter-turn fault. The output of ANN-2 gives 12 classes (F_1–F_{12}) of stator inter-turn faults and ANN-3 gives 6 classes of phase faults and these are as follows:

F_1→ 2-turns short circuit in R phase

F_2→ 4-turns short circuit in R phase

F_3→ 6-turns short circuit in R phase

F_4→ 6-turns short circuit in R phase

F_5→ 2-turns short circuit in Y phase

F_6→ 4-turns short circuit in Y phase

F_7→ 6-turns short circuit in Y phase

F_8→ 8-turns short circuit in Y phase

F_9→ 2-turns short circuit in B phase

F_{10}→ 4-turns short circuit in B phase

F_{11}→ 6-turns short circuit in B phase

F_{12}→ 8-turns short circuit in B phase

P_1→Stator turn-turn fault between RY phases

P_2→Stator turn-turn fault between YB phases

P_3→Stator turn-turn fault between BR phases

P_4→Stator turn-ground fault in R phase

P_5→Stator turn-ground fault in Y phase

P_6→Stator turn-ground fault in B phase

For the simulation of ANN-1, ANN-2 and ANN3 in MATLAB, a tangent sigmoid (tansig)' and log sigmoid (logsig) activation functions are used and training goal is set at 10^{-6}. First, the performance of single multilayer NN of ANN-1 is demonstrated. Various training and testing patterns are generated by using simulation and experimentation. The break up of experimental and simulation data sets of training and testing are given in Table 4. Totally 1287 patterns are carried out to train and test the ANN-1, out of 1287 sets 858 data sets are utilized for training i.e. two third of the total data sets and remaining are used for testing. The training performance of single multilayer NN with respect to number of neurons variation in hidden layer is depicted in Table 5. From Table 5, it is observed that the training accuracy for 12 hidden neurons and 14 hidden neurons are nearly same but number of epochs in 14 neurons is less than 12 neurons. Therefore, for this problem 14 hidden neurons are considered in ANN1.

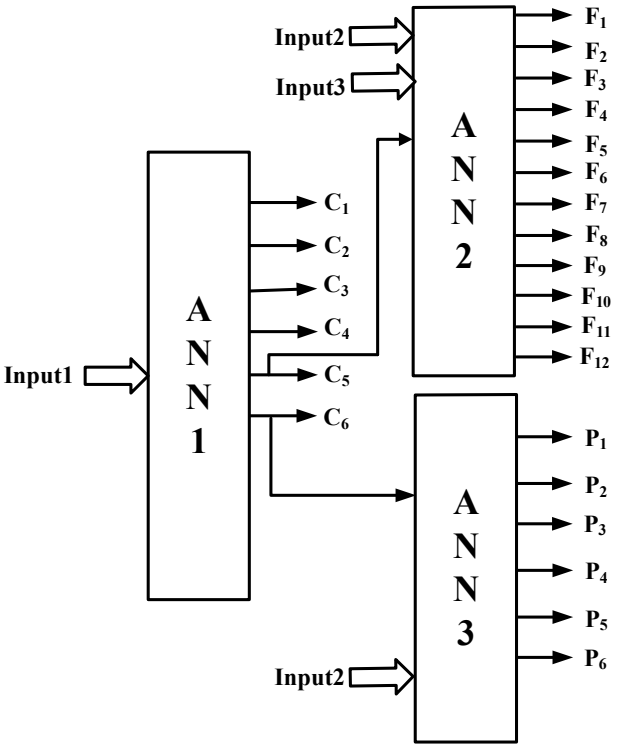

Figure 14. Schematic representation of ANN classifiers.

Table 4. Training and testing data sets for various disturbances.

Type of Disturbance	No. of training patterns		No. of testing patterns	
	Exp	Sim	Exp	Sim
Single Phasing	24	13	12	8
Supply Unbalance	60	54	30	27
Under Voltage	24	23	12	11
Stator Inter-turn fault	72	444	36	222
Sudden load change	18	-	8	-
Phase Faults	18	108	9	54
Total	**216**	**642**	**107**	**322**
	858		**429**	

Table 5. Training performance of single multilayer ANN-1

Number of neurons in hidden layer	Learning epochs	Training accuracy
11	200	96.4%
12	219	97.5%
13	198	97.2%
14	**104**	**97.59%**
15	108	97.13%
16	120	97.4%

In any classifier, the performance evaluation requires specific measures which include accuracy, sensitivity and specificity. Four additional terms are need to know which are used as building blocks in computing many evaluation measures. These are TP (True positives), TN (True negatives), FP (False positives) and FN (False negatives). The confusion matrix is a useful tool for analyzing how well your classifier can recognize tuples of different classes. The accuracy, sensitivity and specificity measures can be used, respectively, for identifying the performance of the classifier. These measures are defined as follows:

$$Sensitivity = \frac{TP}{P} \tag{2}$$

$$Specificity = \frac{TN}{N} \tag{3}$$

$$Accuracy = Sensitivity \frac{P}{(P+N)} + Specificity \frac{N}{(P+N)} = \frac{(TP+TN)}{(P+N)} \tag{4}$$

where $P = TP + FN$ *and* $N = FP + TN$

Table 6. Testing performance of single multilayer ANN-1.

Learning rate	Momentum	Testing accuracy	Training time in sec
0.3	0.67	86.95%	19
0.4		90.21%	14
0.5		88.11%	17
0.6		86.71%	4.07
0.3	**0.68**	86.95%	16
0.4		87.65%	17
0.5		**90.61%**	**7**
0.6		88.11%	7
0.3	**0.69**	86.48%	26
0.4		**90.68%**	**11**
0.5		89.51%	9
0.6		89.74%	9
0.3	0.7	85.05%	18
0.4		85.55%	8
0.5		87.65%	9
0.6		89.04%	16

Table 7. Testing performance of multilayer ANN-1.

No. of neurons in hidden layer1 & 2	Learning rate	Momentum	Testing accuracy	Training time in sec
14, 10	**0.4**	**0.69**	**92.31%**	**37**
14, 20	0.4		90.68%	54
14, 10	0.5	0.68	88.81%	30
14,20	0.5		91.38%	86

The testing performance of ANN-1 is illustrated in Table 6 by making use of different learning rates and different values of momentums. From Table 6 it is observed that for momentum value of 0.69, 0.68 and learning rate of 0.4, 0.5 better accuracy is obtained compared to the remaining. Similarly, same data is used to train and test the multilayer neural network with two hidden layers also and these results are shown in Table 7. From the results, it is proved that the testing accuracy of multilayer neural network is better than single multilayer neural network but the time taken to train the network is more. The output of ANN-1 specifies the stator inter-turn faults, stator phase faults and other faults but not the fault involved phase and severity level. Hence, two more ANNs are used to classify the stator faults along with participated fault phase and to identify the level of fault severity. When the output of ANN-1 indicates the stator inter-turn fault then the classifier two (ANN-2) is activated, if the

fault is a stator phase fault then classifier three (ANN-3) is activated and for other cases ANN-2 and ANN-3 are in an inactive mode. ANN-2 identifies totally 12 types of stator inter-turn faults which are 2, 4, 6 and 8 turn short circuits in R, Y and B phases. The third classifier ANN-3 classifies 6 phase faults such as turn-turn fault between RY phases, turn-turn fault between YB phases, turn-turn fault between BR phases, turn-ground fault in R phase, turn-ground fault in Y phase and turn-ground fault in B phase. Table 8 and Table 9 show the number of training and testing patterns, considered to check the performance of ANN-2 and ANN-3 respectively. Numerous multilayer neural network configurations are carried out by using MATLAB/Simulink software. Among all, the best performance configuration of multilayer network of ANN-2 is 4 (input neurons), 5(hidden neurons), 9 (hidden neurons) and 12 (output neurons). Similarly, for ANN-3 the best performance configuration of multilayer neural network is 3 (input neurons), 5 (hidden neurons), 7 (hidden neurons) and 6 (output neurons). The obtained overall accuracy of the proposed ANN-2 and ANN-3 are 95.74% and 89.39% respectively.

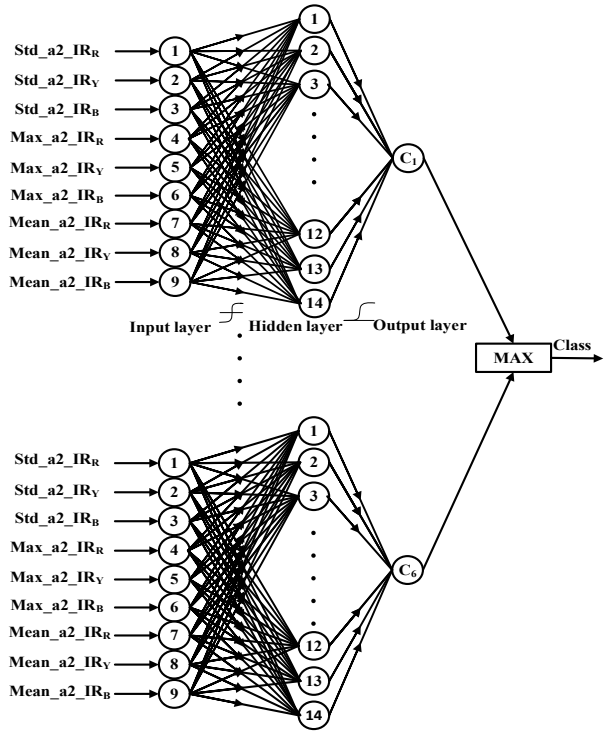

Figure 14. Proposed MNN-1 for disturbance classification.

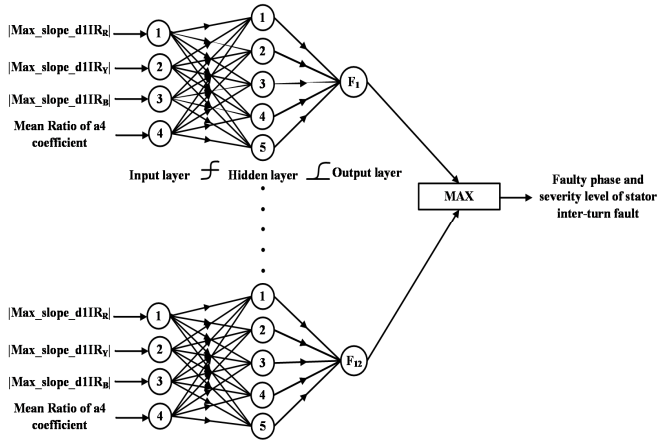

Figure 15. Proposed MNN-2 for classifying the stator phase faults.

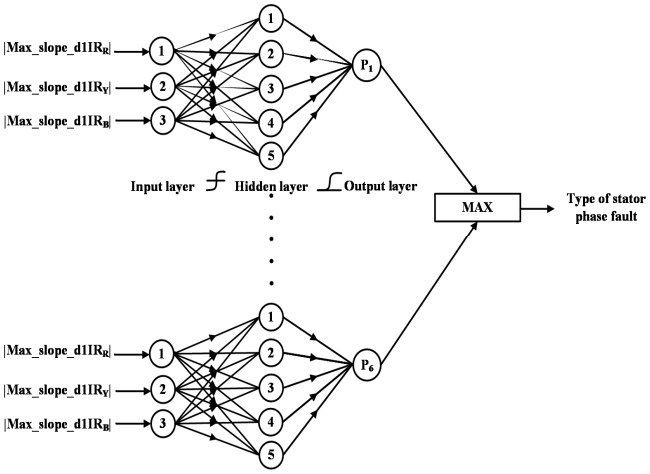

Figure 16. Proposed MNN-3 for identifying the severity level

Table 8. Training and testing patterns for ANN-2

Type of stator inter-turn fault	No. of training patterns		No. of testing patterns	
	Exp	Sim	Exp	Sim
2-turns short in R phase	6	36	3	18
4-turns short in R phase	6	36	3	19
6-turns short in R phase	6	36	3	19
8-turns short in R phase	6	36	3	18
2-turns short in Y phase	6	36	3	18
4-turns short in Y phase	6	36	3	19
6-turns short in Y phase	6	36	3	19
8-turns short in Y phase	6	36	3	18
2-turns short in B phase	6	36	3	18
4-turns short in B phase	6	36	3	19
6-turns short in B phase	6	36	3	19
8-turns short in B phase	6	36	3	18
Total	**72**	**432**	**36**	**222**
	504		**258**	

Table 9. Training and testing patterns for ANN-3.

Type of stator phase fault	No. of training patterns		No. of testing patterns	
	Exp	Sim	Exp	Sim
Stator turn-ground fault in R phase	6	18	2	9
Stator turn-ground fault in Y phase	6	18	2	9
Stator turn-ground fault in B phase	6	18	2	9
Stator turn-turn fault between RY phase	2	19	2	9
Stator turn-turn fault between YB phase	2	19	2	9
Stator turn-turn fault between BR phase	2	19	2	9
Total	**24**	**111**	**12**	**54**

In the proposed work, three modular structures of neural networks (NN) are implemented for classification of various disturbances, classification of stator winding insulation faults and identification of severity level of stator inter-turn faults which are shown in Figure 14, Figure 15 and Figure 16 respectively. Same training and testing data sets are used to check the performance of the modular neural network. Six

types of disturbances have been considered for classification, 6 modules of NN are required to form a modular neural network one (MNN-1). Each module of MNN-1 classifier classifies one class. During training process, features of a particular disturbance signal are applied to all modules with target as "1" to the corresponding neural module and target as "0" to the rest of the modules. During testing, outputs of all the NN modules are compared. The NN modules having largest output will represent the corresponding disturbance class. The performance of classifier of MNN-1 is shown in Table 10. From this table the overall accuracy of the modular classifier of MNN-1 is 94.64% and this performance is achieved within 4 sec. Hence, the results proved that the performance of MNN-1 is significantly higher (2.4%) as compared to multilayer neural network classifier of ANN-1. The output of MNN-1 specifies the stator inter-turn faults, stator phase faults and other faults but not the fault involved phase and severity. Hence, two more modular structures of NNs are used to classify the stator winding insulation faults along with participated fault phase and severity level. When the output of MNN-1 indicates the stator inter-turn fault (C_5 becomes 1) then MNN-2 is activated. If the output of MNN-1 indicates stator phase fault, then MNN-3 is activated. Each module of MNN-2 classifier indicates the 4 levels of inter-turn severities in R-phase, Y-phase and B phase. The other stator winding insulation faults such as ground and phase-phase faults are classified by MNN-3. The testing performance of MNN-2 and MNN-3 are illustrated make use of confusion matrix. Tables 11 and 12 demonstrate the overall accuracy of the MNN-2 and MNN-3 respectively. The results demonstrate that the overall accuracy of the classifiers of MNN-2 and MNN-3 are improved by 1.16% and 4.55% respectively when compared with multilayer neural network classifiers. The number of iterations required for archiving the best accuracy in ANN-2, ANN-3, MNN-2 and MNN-3 are 609, 453, 192, and 47 iterations respectively. All the modular classifiers together has to be taken within 6 sec for training the networks.

The other performance measures associated with classifier are the sensitivity and specificity. Table 13 demonstrates the values of sensitivity and specificity for ANN-1 and MNN-1 based classifiers corresponding to 6 types of disturbances. Similarly Tables 14 and 15 show the values of sensitivity and specificity of the classifiers ANN-2 vs MNN-2 and ANN-3 vs MNN-3 respectively. From the Tables 13, 14 and 15, it is clear that the modular structure of neural network has more capability to classify the disturbances, types of stator winding insulation faults and severity level of stator inter-turn faults. Hence the modular based classifiers are significantly far better than the multilayer neural network classifier.

Table 10. Confusion matrix for MNN-1.

	C_1	C_2	C_3	C_4	C_5	C_6
C_1	21	0	0	0	0	0
C_2	2	50	0	0	3	1
C_3	0	0	22	0	0	1
C_4	0	0	0	9	1	0
C_5	1	4	2	2	246	1
C_6	0	2	0	2	1	58
Overall accuracy = 94.64 %						

Table 11. Confusion matrix for MNN-2.

	F_1	F_2	F_3	F_4	F_5	F_6	F_7	F_8	F_9	F_{10}	F_{11}	F_{12}
F_1	21	0	0	0	0	0	0	0	0	0	0	0
F_2	0	21	1	0	0	0	0	0	0	0	0	0
F_3	0	0	22	0	0	0	0	0	0	0	0	0
F_4	0	0	0	21	0	0	0	0	0	0	0	0
F_5	0	0	0	0	20	0	0	0	0	1	0	0
F_6	0	0	0	0	0	22	0	0	0	0	0	0
F_7	0	0	0	0	0	2	20	0	0	0	0	0
F_8	0	0	1	0	0	0	0	20	0	0	0	0
F_9	0	0	0	0	0	1	0	0	20	0	0	0
F_{10}	0	0	0	0	0	0	0	0	0	22	0	0
F_{11}	0	0	0	0	0	0	0	0	0	2	20	0
F_{12}	0	0	0	0	0	0	0	0	0	0	0	21
Overall accuracy = 96.9%												

Table 12. Confusion matrix for MNN-3

	P_1	P_2	P_3	P_4	P_5	P_6
P_1	11	0	0	0	0	0
P_2	0	11	0	0	0	0
P_3	2	0	11	0	0	0
P_4	0	0	0	10	0	0
P_5	0	0	0	0	10	0
P_6	0	0	0	2	0	9
Overall accuracy = 93.94%						

Table 13. Performance for ANN-1 and MNN-1 in disturbance classification

Type of network	Type of disturbance	Sensitivity	Specificity	Average Values
ANN-1	C_1	0.952	0.995	Sensitivity: 0.858
	C_2	0.804	0.989	
	C_3	0.913	0.980	
	C_4	0.961	0.942	Specificity: 0.98
	C_5	0.6	0.998	
	C_6	0.921	0.978	
MNN-1	C_1	1	0.993	Sensitivity: 0.939
	C_2	0.893	0.984	
	C_3	0.957	0.995	
	C_4	0.961	0.971	Specificity: 0.987
	C_5	0.9	0.99	
	C_6	0.921	0.992	

Table 14. Performance for ANN-2 and MNN-2 in stator faults classification.

Type of network	Type of fault	Sensitivity	Specificity	Average Values
ANN-2	F_1	1	1	Sensitivity: 0.958
	F_2	0.956	0.996	
	F_3	1	1	
	F_4	1	1	
	F_5	0.952	1	
	F_6	1	0.987	
	F_7	0.909	1	Specificity: 0.996
	F_8	1	0.996	
	F_9	0.905	0.996	
	F_{10}	0.954	0.983	
	F_{11}	0.864	0.995	
	F_{12}	0.952	1	
MNN-2	F_1	1	1	Sensitivity: 0.969
	F_2	0.956	1	
	F_3	1	0.992	
	F_4	1	1	
	F_5	0.952	1	
	F_6	1	0.987	
	F_7	0.909	1	Specificity: 0.997
	F_8	0.952	1	
	F_9	0.952	1	
	F_{10}	1	0.987	
	F_{11}	0.909	1	
	F_{12}	1	1	

Table 15. Performance for ANN-3 and MNN-3 in stator phase faults classification

Type of network	Type of stator phase fault	Sensitivity	Specificity	Average Values
ANN-3	P_1	0.909	0.964	Sensitivity: 0.896
	P_2	1	0.964	
	P_3	0.846	0.981	
	P_4	1	0.964	Sensitivity: 0.979
	P_5	0.8	1	
	P_6	0.818	1	
MNN-3	P_1	1	0.964	Sensitivity: 0.944
	P_2	1	1	
	P_3	0.846	1	
	P_4	1	0.964	Sensitivity: 0.988
	P_5	1	1	
	P_6	0.818	1	

7 CONCLUSION

In this paper an attempt has been made to extract efficient features of the induction motor disturbances using SWT and DWT. The observations made from the results indicate that the SWT has clear advantage over the DWT to extract the fault residues in the presence of noise and supply unbalances. The developed simulation model is validated through experimental setup and the frequency responses obtained from the simulated model closely matches with the experimental setup. The instant at which disturbance starts can be identified by comparing the fault indices with adaptive threshold and count value. The threshold based reconstruction and adaptive threshold logic have improved the effectiveness of the proposed detection scheme. By introducing modular concept to NN for disturbance classification, stator winding insulation faults classification and level of severity identification, the task complexity is reduced and learning capability is increased. It is observed from the results that the performance of MNN-1 is significantly higher as compared to that of ANN-1 and the same trend is followed in both the cases of MNN-2 and MNN-3 classifiers. Similarly, the training time required for modular neural network is less compared with ANN. This diagnosis approach improves the efficacy as the features required for detection and classification are obtained over a window of one cycle from the point of disturbance. Hence the proposed technique is effective in detecting and classifying the stator winding insulation faults and severity level of inter-turn faults with a minimum time.

REFERENCES

[1] A. Siddique, G. Yadava, and B. Singh, "A review of stator fault monitoring techniques of induction motors," IEEE Trans. Energy Conversion, Vol. 20, No. 1, pp. 106-114, 2005.

[2] M. Rangarajan Tallam, Sang Bin Lee, C. Greg Stone, G. B. Kliman, Jiyoon Yoo, G. Thomas Habetler, and G. Ronald Harley, "A survey of methods for detection of stator-related faults in induction machines", IEEE Trans. Ind. Appl., Vol. 43, No.4, pp. 920-933, 2007.

[3] P. Zhang, Y. Du, G. Thomas Habetler, and Bin Lu. "A survey of condition monitoring and protection methods for medium-voltage induction motors", IEEE Trans. Ind. Appl., Vol. 47, No. 1, pp. 34-46, 2011.

[4] G. Stefan, M. Jose Aller, B. Lu, and G. T. Habetler, "A survey on testing and monitoring methods for stator insulation systems of low-voltage induction machines focusing on turn insulation problems", IEEE Trans. Ind. Electron., Vol. 55, No. 12, pp. 4127-4136, 2008.

[5] S. Nandi, H. A. Toliyat, and X. Li, "Condition monitoring and fault diagnosis of electrical motors-a review", IEEE Trans. Energy Convers., Vol. 20, No. 4, pp. 719-729, 2005.

[6] G. B. Kliman, W. J. Premerlani, R. A. Koegl, and D. Hoeweler, "A new approach to on-line turn fault detection in ac motors", Conf. Rec. 31st, IEEE IAS Annual Meeting, Vol. 1, pp. 687-693, 1996.

[7] S. M. Cruz, and A. M. Cardoso, "Stator winding fault diagnosis in three-phase synchronous and asynchronous motors, by the extended park's vector approach", IEEE Trans. Ind. Appl., Vol. 37, No. 5, pp. 1227-1233, 2001.

[8] A. M. Da Silva, R. J. Povinelli, and N. A. Demerdash, "Induction machine broken bar and stator short-circuit fault diagnostics based on three-phase stator current envelopes", IEEE Trans. Ind. Electr., Vol. 55, No. 3, pp. 1310-1318, 2008.

[9] S. M. A. Cruz, and A. J. M. Cardoso, "Multiple reference frames theory: A new method for the diagnosis of stator faults in three-phase induction motors," IEEE Trans. Energy Convers., Vol. 20, No. 3, pp. 611-619, 2005.

[10] J. Cusido, L. Romeral, J. A. Ortega, J. A. Rosero, and A. Garcia Espinosa, "Fault detection in induction machines using power spectral density in wavelet decomposition," IEEE Trans. Ind. Electron., Vol. 55, No. 2, pp. 633-643, Feb. 2008.

[11] S. Nandi, and H. A. Toliyat, "Novel frequency-domain-based technique to detect stator inter turn faults in induction machines using stator-induced voltages after witch-off", IEEE Trans. Ind. Appl., Vol. 38, No.1, pp. 101-109, 2002.
[12] A. Gandhi, T. Corrigan, and L. Parsa, "Recent advances in modeling and online detection of stator inter turn faults in electrical motors", IEEE Trans. Ind. Electron., Vol. 58, No. 5, pp.1564-1575, 2011.
[13] D. C. Patel, and M. C. Chandorkar, "On-line load test for induction machine stator inter-turn fault detection under stator electrical asymmetries", IEEE 36th Annual Conf. Ind. Elect., IECON-2010, pp. 933-937, 2010.
[14] J. Yun, K. Lee, K. W. Lee, S. B. Lee, and J. Y. Yoo, "Detection and classification of stator turn faults and high resistance electrical connections for induction machines", IEEE Trans. Ind. Appl., Vol. 45, No. 2, pp. 666-675, 2009.
[15] M. Ghazal, and J. Poshtan, "Robust stator winding fault detection in induction motors", Power Electronics, Drive Systems and technologies conf. pp. 163-168, 2011.
[16] S. Das, C. Koley, P. Purkait, and S. Chakravorti, "Performance of a Load-Immune Classifier for Robust Identification of Minor Faults in Induction Motor Stator Winding", IEEE Trans. Dielect. Electr. Insul., Vol. 21, No. 1, pp. 33-44, 2014.
[17] M. A. Awadallah, and M. M. Morcos, "Application of AI tools in fault diagnosis of electrical machines and drives-an overview", IEEE Transactions on Energy Conversion, Vol. 18, No. 2, pp. 245-251, 2003.
[18] X. Z. Gao, and S. J. Ovaska, "Soft computing methods in motor fault diagnosis", Applied soft computing, Vol. 1, No.1, pp. 73-81, 2001.
[19] M. Ghazal, and J. Poshtan, "Robust stator winding fault detection in induction motors", Proc. Power Electronics, Drive Systems and technologies conf. pp. 163-168, 2011.
[20] M. S. Ballal, Z. J. Khan, H. M. Suryawanshi, and R.L. Sonolikar, "Adaptive Neural Fuzzy Inference system for the detection of inter-turn insulation and bearing wear faults in induction motor", IEEE Trans. Ind. Appl., Vol. 54, No. 1, pp. 250-258, 2007.
[21] S. Altug, M. Y. Chen, and H. J. Trussell, "Fuzzy Inference systems implemented on Neural architectures for motor fault detection and diagnosis", IEEE Trans. Ind. Appl., Vol. 46, No. 6, pp. 1069-1079, 1999.
[22] P. Akhlaghi, A. R. Kashanipour, and K. Salahshoor, "Complex dynamical system fault diagnosis based on multiple ANFIS using independent component", 16th Mediterranean Conf. on Control and Automation, Ajaccio, France, pp. 1798-1803, 2008.
[23] P. V. Goode, and M. Y. Chow, "Using a neural/fuzzy system to extract heuristic knowledge of incipient faults in induction motors: Part I and II", IEEE Trans. Ind. Electron., Vol. 42, No. 2, pp. 131-146, 1995.
[24] G. Auda, M. Kamel, and H. Raafat, "Modular neural architectures for classification", IEEE Intl. Conf. Neural Networks, Vol. 2, pp.1279-1284, 1996.
[25] B. L. Lu, and M. Ito, "Task decomposition and module combination based on class relations: a modular neural network for pattern classification", IEEE Trans. Neural Networks, Vol. 10, No. 5, pp. 1244-1256, 1999.
[26] B. Mirafzal, G. L. Skibinski, R. M. Tallam, D. W. Schlegel, and R. A. Lukaszewski, "Universal induction motor model with low-to-high frequency-response characteristics", IEEE Trans. Ind. Appl., Vol. 43, No. 5, pp. 1233-1246, 2007.
[27] O. A. Youssef, "Online applications of wavelet transforms to power system relaying", IEEE Trans. Power Delivery, Vol. 18, No. 4, pp. 1158-1165, 2003.
[28] H. A. Darwish, M. Hesham, A. M. I. Taalab, and N. M. Mansour, "Close accord on DWT performance and real-time implementation for protection applications", IEEE Trans. Power Delivery, Vol. 25, No. 4, pp. 2174-2183, 2010.
[29] T. Hong, M. T. C. Fang, and D. Hilder, "PD classification by a modular neural network based on task decomposition", IEEE Trans. Dielectr. Electr. Insul, Vol. 3, No. 2, pp. 207-212, 1996.
[30] U. Lahiri, A. K. Pradhan, and S. Mukhopadhyaya. "Modular neural network-based directional relay for transmission line protection", IEEE Trans. Power Systems, Vol. 20, No. 4, pp. 2154-2155, 2005.

N. Rama Devi received the B.Tech. degree in electrical and electronics engineering from J.N.T.U. Engineering College, Kakinada, India in 1997, and the M.Tech degree in power systems from the Regional Engineering College, Warangal, India, in 2000. She is working as Associate Professor in the Department of Electrical and Electronics Engineering at Bapatla Engineering College, Bapatla,India since 2006. Presently, she is pursuing Ph.D. degree at the National Institute of Technology, Warangal, India.

D.V.S.S. Siva Sarma received his BTech in EEE and MTech in power systems from JNTU College of Engineering, Anantapur in 1986 and 1988, respectively. He received his doctorate degree from the Indian Institute of Technology, Madras in 1993. He joined the National Institute of Technology, Warangal, India in 1992. Presently, he is a Professor in the Department of Electrical Engineering. He acted as a Chair- Student Activities, IEEE Hyderabad Section during 2009-2011 and received IEEE Outstanding Branch Counselor & Advisor Award in 2009. He served as a Vice Chair, PES/IAS/PELS Joint Chapter, IEEE Hyderabad Section for 2011 and Chair, PES/IAS/PELS Joint Chapter of IEEE Hyderabad Section for 2012. Currently, he is the Chairman of Indian EMTP User Group, Senior member in IEEE, and Fellow of Institution of Engineers. His areas of interest include power system transients, power quality, protection and condition monitoring of power apparatus and EMTP applications.

P.V. Ramana Rao graduated from the Indian Institute of Technology, Madras, India in 1967 and received the M.Tech degree from the Indian Institute of Technology, Kharagpur, India in 1969. He obtained his Ph.D. degree from the Regional Engineering College, Warangal, India in 1982. He handled many positions in the Department of Electrical Engineering at National Institute of Technology, Warangal, India during 1982-2010. He received best teacher award in 2004 given by the State Govt AP. Currently, he is working as Professor and head of Electrical and Electronics Engineering at ANU College of engineering and technology, Guntur, India. Presently, he is a senior member in IEEE. His areas of interest are Power System Stability, Power System Protection, and HVDC Transmission.